Structural insight into acute intermittent porphyria

Gaojie Song,* Yang Li,* Chongyun Cheng,* Yu Zhao,* Ang Gao,* Rongguang Zhang,[†] Andrzej Joachimiak,[†] Neil Shaw,*,[1] and Zhi-Jie Liu*,[1]

*National Laboratory of Biomacromolecules, Institute of Biophysics, Chinese Academy of Sciences, Beijing, China; and [†]Structural Biology Center, Advanced Photon Source, Argonne National Laboratory, Argonne, Illinois, USA

ABSTRACT **Acute intermittent porphyria (AIP), an inherited disease of heme biosynthesis, is one of the most common types of porphyria. Reduced activity of the enzyme porphobilinogen deaminase (PBGD), which catalyzes the sequential condensation of 4 molecules of porphobilinogen to yield preuroporphyrinogen, has been linked to the symptoms of AIP. We have determined the 3-dimensional structure of human PBGD at 2.2 Å resolution. Analysis of the structure revealed a dipyrromethane cofactor molecule covalently linked to C261, sitting in a positively charged cleft region. In addition to the critical catalytic D99, a number of other residues are seen hydrogen bonded to the cofactor and play a role in catalysis. Sequential entry of 4 pyrrole molecules into the active site is accomplished by movement of the domains around the hinges. H120P mutation resulted in an inactive enzyme, supporting the role of H120 as a hinge residue. Interestingly, some of the mutations of the human PBGD documented in patients suffering from AIP are located far away from the active site. The structure provides insights into the mechanism of action of PBGD at the molecular level and could aid the development of potential drugs for the up-regulation of PBGD activity in AIP.—Song, G., Li, Y., Cheng, C., Zhao, Y., Gao, A., Zhang, R., Joachimiak, A., Shaw, N., Liu, Z.-J. Structural insight into acute intermittent porphyria. *FASEB J.* 23, 396–404 (2009)**

Key Words: human porphobilinogen deaminase · X-ray structure · heme biosynthesis · porphobilinogen hinge

HEME, AN IRON-CONTAINING TETRAPYRROLE, is vital for the survival and propagation of all living cells. In its role as a prosthetic group for hemoglobin, heme is involved in the binding and transport of oxygen (1, 2). Other basic cellular processes that involve heme include electron transfers during respiration and the complex redox reactions catalyzed by cytochrome P-450 (2). Heme biosynthesis in mammals is accomplished by the sequential action of 8 enzymes (3–7). Except for the first enzyme, aminolaevulinic acid synthase, deficiency in any one of the remaining 7 enzymes results in a metabolic disorder termed porphyria (3, 4, 7, 8). Decreased activity of the third enzyme in the heme biosynthetic pathway—porphobilinogen deaminase (PBGD; EC 4.3.1.8), also known as 1-hydroxymethylbi-

lane synthase or uroporphyrinogen I synthase—causes acute intermittent porphyria (AIP) (9–11). AIP is the most common type of porphyria, characterized by the accumulation of high amounts of porphyrin precursors, such as δ-aminolaevulinic acid (ALA) and porphobilinogen (PBG), leading to gastrointestinal disturbances, seizures, neurological dysfunctions, and hepatic carcinoma. The most common signs and symptoms of AIP include acute abdominal pain, nausea, vomiting, constipation, and tachycardia. Exposure to other precipitating factors, such as starvation, drugs, hormones, infection, alcohol, or stress, could lead to a potentially life-threatening state of acute attacks (8, 12).

In humans, at least two isoforms of PBGDs have been reported: the 44-kDa housekeeping enzyme and the 42-kDa erythrocyte-specific enzyme (13). The ubiquitous PGBD polypeptide consists of 361 amino acid residues, while the erythroid variant is made up of 344 amino acids. The housekeeping PBGD has 17 additional amino acids at the N terminus, the function for which is not clear yet (13). PBGDs are highly conserved across different species and exist as monomers with a mass ranging from 34 to 45 kDa, depending on the species (14). PBGD catalyzes the sequential polymerization of four molecules of porphobilinogen to form l-hydroxymethylbilane, also known as preuroporphyrinogen. Catalysis begins with the assembly of the dipyrromethane cofactor by the apoenzyme from two molecules of porphobilinogen or from preuroporphyrinogen. The covalently linked cofactor acts as a primer, around which the tetrapyrrole product is assembled. In the last step of catalysis, the product, preuroporphyrinogen, is released, leaving the cofactor bound to the holodeaminase intact. The 4 covalent enzyme-intermediate complexes, ES1, ES2, ES3, and ES4, which are sequentially generated during the course of the tetrapolymerization, have different degrees of stability and have been isolated and characterized extensively (15, 16).

The 3-dimensional (3-D) structure of PBGD from *Escherichia coli* has been solved using X-ray crystallogra-

phy (17). PBGDs from humans share over 45% primary sequence identity with their counterparts from *E. coli* and other species. However, no experimental structures of PBGDs from other organisms have been reported so far. Therefore, it is not clear yet whether the structure of PBGD from *E. coli* is totally conserved in other species and whether the proposed mechanism is universally applicable to eukaryotic PBGDs. More important, in order to develop potential drugs that can up-regulate the activity of PBGD during diseased states, the knowledge of structure and catalytic mechanism of human PBGD is necessary. Hence, we report the crystal structure of human porphobilinogen deaminase bound with dipyrromethane cofactor solved at 2.2 Å resolution. We have mapped the location of amino acid substitutions documented in patients suffering from AIP on the 3-D structure of PBGD and probed their effect on the structure and function of the enzyme.

MATERIALS AND METHODS

Protein expression and purification

A 1086-base pair DNA fragment coding PBGD was amplified using forward primer 5′-TACTTCCAATCCAATGCTATGTC-TGGTAACGGC-3′ and reverse primer 5′-TTATCCACTTC-CAATGTTAATGGGCATCGTTAAG-3′. The resulting DNA fragment was ligated into vector pMCSG7 (18) and transformed into *E. coli* BL21(DE3) cells. The cells were cultured in Luria-Bertani (LB) medium containing ampicillin (100 μg/ml) at 37°C until OD_{600nm} reached 0.8. The culture was then induced with 0.2 mM isopropyl-β-D-thiogalactoside (IPTG) for 20 h at 16°C. Cells were harvested by centrifugation, lysed by sonication, and clarified by centrifugation; the supernatant was then applied to a nickel-nitrilotriacetic acid (Ni-NTA) resin gravity column (Qiagen, Valencia, CA, USA) that had been previously equilibrated with PBS (137 mM NaCl, 2.7 mM KCl, 50 mM Na_2HPO_4, 10 mM KH_2PO_4, pH 7.4). The column was first washed with 100 ml PBS, followed by washing with 100 ml PBS containing 20 mM imidazole, and finally eluted with PBS containing 300 mM imidazole. After buffer exchange, the His-tag was cleaved by tobacco etch virus (TEV) treatment. Uncut protein was separated by Ni-affinity chromatography. PBGD was further purified using a Hitrap Q FF ion-exchange chromatography column (Amersham, Piscataway, NJ, USA) equilibrated with buffer A (20 mM Tris-HCl, pH 7.5). After rigorous washing with buffer A, bound PBGD was eluted using a linear gradient of 0 to 0.5 M NaCl in buffer A. Fractions containing the protein were pooled, concentrated, and loaded on Superdex G75 size-exclusion chromatography column (Amersham) equilibrated with 20 mM Tris-HCl, pH 8.0, and 200 mM NaCl. Fractions containing the protein were pooled and concentrated to 15 mg/ml before setting up crystallization trials.

PBGD assay

PBGD activity was determined as described previously (16). Briefly, the reaction mixture contained 20 μM porphobilinogen in 0.1 M Tris-HCl, pH 8.0, and 0.1 M dithiothreitol (DTT) in a final volume of 300 μl. PBGD was added to initiate the reaction, and the mixture was incubated at 37°C for 10 min. At the end of the incubation time, the reaction was stopped by the addition of 50 μl of 5 M HCl. The contents

were then exposed to light for 1 h in order to oxidize the uroporphyrinogen to uroporphyrin. Absorbance was read at 405.5 nm. One unit of PBGD activity was defined as the amount of enzyme required to produce 1 nmol of uroporphyrin in 1 h at 37°C under the assay conditions.

Site directed mutagenesis

Site-directed mutagenesis of PBGD was carried out using the QuikChange site-directed mutagenesis kit (Stratagene, La Jolla, CA, USA). Reactions were set up according to the manufacturer's instructions. The entire length of the genes was sequenced in order to verify the mutations. Mutants were expressed and purified the same way as the wild-type enzyme and assayed for activity under identical conditions.

Crystallization and structure solution

Crystallization screening was done with the Mosquito™ robot (TTP LabTech Ltd., Royston, UK) using commercially available sparse matrix screens. Diffraction-quality crystals were produced at 16°C in a mother-liquor solution containing 0.15 M ammonium citrate dibasic and 22% (w/v) PEG3350. Single crystals were frozen in liquid nitrogen prior to X-ray diffraction testing and data collection. Diffraction data were collected at a wavelength of 0.9794 Å at beamline 19-ID, Advanced Photon Source, Argonne National Laboratory. All data sets were collected at cryogenic temperature. The data were indexed, integrated, and scaled using HKL2000 (19). The initial model and phase were obtained by molecular replacement using Balbes (20). Phenix.autobuild (21) was used to rebuild the model with the initial phase. The model was manually improved in Coot (22), and Oasis MR iteration (unpublished results) was used to improve the phase. Alter-

TABLE 1. *Data collection and refinement statistics*

Statistic	Native
Data collection	
Space group	$P2_12_12_1$
Cell dimensions	
a, b, c (Å)	71.61, 81.06, 109.21
α, β, γ (°)	90.00, 90.00, 90.00
Resolution (Å)	50–2.2
R_{sym}	0.12 (0.45)
$I/\sigma I$	13.94 (2.25)
Completeness (%)	88.9 (55.5)
Redundancy	6.0 (4.7)
Refinement	
Resolution (Å)	38.27–2.18
No. reflections	29,562
R_{work}/R_{free}	0.2317/0.2714
No. atoms	
Protein	4771
Water	138
B-factor	
Protein	20.32
Water	56.48
Root mean square deviation	
Bond lengths (Å)	0.010
Bond angles (°)	1.309

Highest-resolution shell is shown in parenthesis.

nate cycles of Phenix.refine (21), and manual adjustments resulted in the final model, with statistics listed in **Table 1**. During refinement, thinshell was used to choose the free sets due to the translation NCS located in the asymmetric unit.

RESULTS

Overall structure

Human PBGD crystallized in $P2_12_12_1$ space group with two molecules packed in the asymmetric unit. The monomers of each dimer are related by a noncrystallographic translation symmetry. Although a solvent content of 38% indicated that PBGD exists as a dimer in the asymmetric unit, the size-exclusion profile showed that the enzyme behaves as a monomer in solution. Dimerization of PBGD may have occurred, possibly due to crystal-packing preferences. Electron density for most of the polypeptide was of good quality, except for a few residues in loop regions: amino acids M1–M18, S57–S76, G259, S262, V263, L357-H361 of chain A; and residues M1-M18, S57-K70, V301-D312, Q356-H361 of chain B could not be traced.

The human PBGD is comprised of 3 distinct domains (**Fig. 1A**). The N-terminal domain 1, residues 1-116 and 216-239, is made up of 3 antiparallel and 2 parallel β-sheets surrounded by 3 helices. In addition, domain 1 consists of numerous loops. The loop region made up of residues S57–S76 is in proximity to the active site. Although the electron density for this region is missing, it could be modeled using Geno 3D (23). The model revealed this loop region to be forming a cap-like structure that covers the active site (Fig. 1A). Residues 117-215 make up domain 2. The arrangement of the secondary structure elements for domain 2 is almost similar to that of domain 1. The hydrophobic core of domain 2 is made up of 5 β-sheets, 3 of which run antiparallel. The sheets are surrounded by 5 helices, 2 of which are short 3_{10}-helices. The active site is located in a cleft region between domains 1 and 2. Residues 240-361 form the C-terminal domain 3. Three long antiparallel β-sheets and 3 helices make up domain 3. The critical residue, C261, that covalently binds the dipyrromethane cofactor molecule is located in a loop region (residues 248-264), which is part of domain 3.

The overall structure of human PBGD closely mirrors that of the enzyme structure reported from *E. coli* (17). Superimposition studies revealed a root mean square deviation of 1.16 Å for 279 (of 361) overlapping Cα positions. A notable feature of the human PBGD is the presence of 20 amino acids (I299-I318) at the C terminus, which are absent in the enzyme from *E. coli*. These amino acids are part of domain 3 and are seen forming a loop at the interface of domains 1 and 3. This loop may be involved in stabilizing the conformations of the enzyme but does not seem to be necessary for the function of the enzyme in *E. coli*.
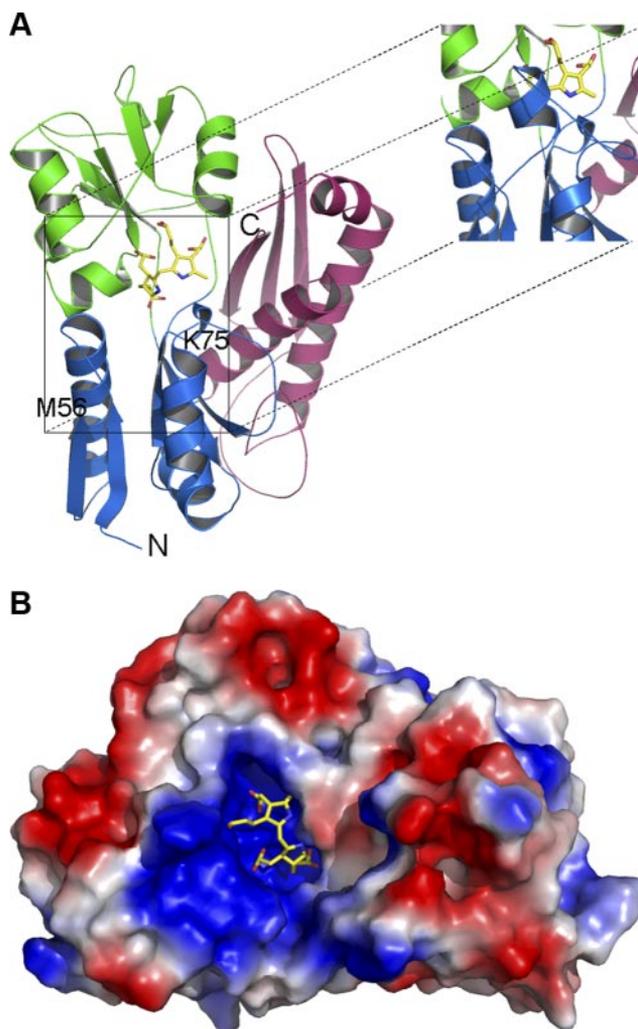
Figure 1. Overall structure of human PBGD. *A*) Cartoon representation of human PBGD bound with dipyrromethane cofactor. Domain 1 is blue, domain 2 is green, and domain 3 is purple. N and C terminals of protein are marked as N and C, respectively. Residues S57-S76 were modeled using Geno 3D (see inset). *B*) Surface electrostatic potential representation of human PBGD. Blue, positive potential; red, negative potential. Cofactor is shown as sticks.

Active site

The active site is located at the interface of domains 1 and 2. The dipyrromethane cofactor molecule covalently linked to C261 is seen sitting in a large positively charged cleft region (Fig. 1*B*). The cleft is large enough to accommodate more molecules of methylene pyrrolinene during catalysis. Electron density for the dipyrromethane cofactor was very well defined. The C1 and C2 rings of the cofactor along with its side chains could be modeled accurately (**Fig. 2**). The C1 ring of the cofactor is linked to C261 *via* a covalent bond. A number of residues are seen forming hydrogen bonds with the cofactor. The interactions are predominantly ionic, with positively charged residues like K98, R149, R150, R173, R195, and Q217 interacting with the carboxyl oxygens of the cofactor (Fig. 2). Interestingly, all of these residues are totally conserved in PBGDs
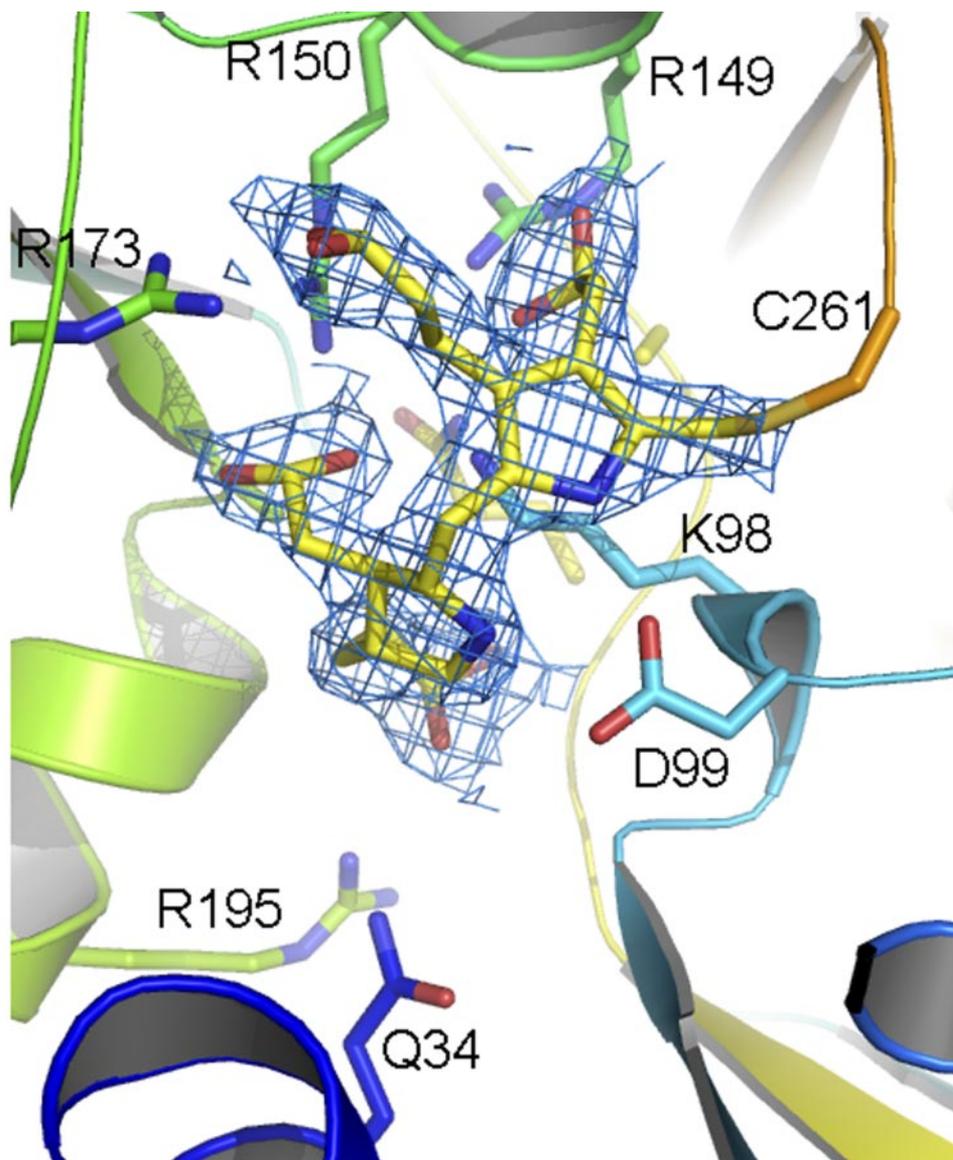
Figure 2. Active site of human PBGD. A number of charged residues are seen forming ionic interactions with the dipyrromethane cofactor. The cofactor omitted F_o-F_c electron density was contoured at 2σ. Interacting residues and the cofactor are represented as sticks.

from different species, indicating a highly conserved mechanism of substrate binding and catalysis (17) (Supplemental Fig. 1 and **Fig. 3**). Such interactions probably help in docking the cofactor and neutralize the charges. The key residue for catalysis, D99, is within hydrogen bonding distance of the pyrrole nitrogens. These features are reminiscent of the active site of PBGD from *E. coli* (17).

Alignment of primary sequences of PBGDs from different sources revealed a number of highly conserved residues around the active site, indicating a common mechanism of action across different species (Supplemental Fig. 1). The K_m values reported for PBGDs from various sources fall in a narrow range of 15–20 μM (24–28). Interestingly, the PBGD isoenzyme isolated from human erythrocytes lacks the first 17 amino acids found in the housekeeping PBGD used in this study but showed similar K_m values toward porphobilinogen when compared to the housekeeping PBGD (29). The PBGD for the current study was amplified from the human liver cDNA library. The K_m value for

this PBGD was 15 μM when assayed under similar conditions reported for PBGDs from other sources (**Fig. 4**). This shows that the structural conservation between different species seems to be quite stringent.

Mechanism of catalysis

The holoenzyme of PBGD contains a dipyrromethane cofactor covalently linked to C261. The assembly of this cofactor begins with the deamination of a porphobilinogen molecule to yield methylene pyrrolinene, followed by its reaction with the deprotonated sulfydryl group of C261. A second molecule of the methylene pyrrolinene is added in similar fashion, except this time the nucleophilic attack is mounted by the free α-position of the ring already attached to C261 (**Fig. 5**). The dipyrromethane cofactor assembled in the active site is bound permanently to the enzyme and acts as a primer around which the tetrapyrrole product is synthesized. Alternatively, preuroporphyrinogen has been reported as the initial source of the cofactor (30). Pyrrole rings are
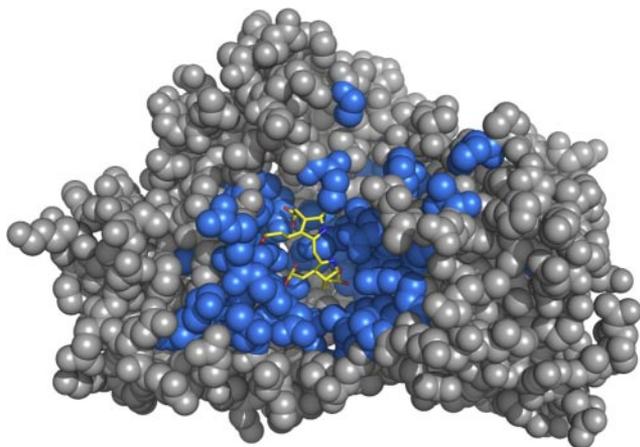
Figure 3. Absolutely conserved residues of PBGD from different species are shown as blue balls. The dipyrromethane cofactor is shown as sticks. Most of the absolutely conserved residues are centered around the active site.

added sequentially by deamination of porphobilinogen, followed by the formation of carbon-carbon bond between the methylene pyrrolinene and the free α position of the terminal ring bound to the enzyme. The reaction proceeds through ES1, ES2, ES3, and ES4 intermediate states with the addition of a pyrrole ring at each stage. Steric considerations prevent the addition of more rings beyond the ES4 tetrapyrrole stage. The reaction is then terminated by the release of the product, preuroporphyrinogen. Product release is accomplished by a process that is exactly the reverse of the ring-coupling reaction. The α-position of the C2 ring of the dipyrromethane cofactor is protonated followed by the cleavage of the carbon-carbon bond and the subsequent nucleophilic attack mounted by a water molecule completes product formation (31).

The dipyrromethane cofactor bound to the enzyme could help identify the critical residues for catalysis (**Fig. 6***A*). D99 is well positioned to promote the catalysis. In the case of PBGD from *E. coli*, D84 occupies a similar position as D99 in human PBGD (17). The phenyl ring of F62 has been postulated to protonate the aspartate carboxyls in case of PBGD from *E. coli*. An equivalent phenylalanine residue in human PBGD, F77, is far away from the aspartate and is unlikely to protonate the carboxyl oxygens. Analysis of the active site revealed R26, Q34, or R195 positioned close to the C2 ring of the cofactor and potentially able to protonate the amine group of the incoming porphobilinogen molecule instead of D99 (Fig. 6*A*). Mutation of R26, Q34, or R195 to alanine results in an inactive PBGD (**Table 2**). Such mutations probably compromise the ability of these residues to protonate the porphobilinogen. The O4B carboxyl oxygen on the propionate side chain of the C2 ring of the cofactor is not hydrogen bonded to any other residue and is seen interacting with NH1 nitrogen of R195 through a weak 3.7 Å Wan der Waals interaction (Fig. 6*B*). This oxygen is well positioned to donate electrons and stabilize the positive charge developed on the incoming pyrrole nitrogen.

The carboxyl oxygen of D99 is seen forming a hydrogen bond with the nitrogen atom of the C2 ring of the cofactor (Fig. 6*A*). This interaction results in the relay of charge to the carbon at the α position, which can now mount a nucleophilic attack and form a carbon-carbon bond with the new methylene pyrrolinene ring. After the new bond formation, D99 abstracts the electrons from the α-position of the C2 ring attached to the cofactor, thus stabilizing the intermediate. D99G mutants of human PBGD (D84A in *E. coli* PBGD) have been reported to accumulate inactive ES2 complexes (31, 32). This result suggests that the initial source of dipyromethane cofactor could be preuroporphyrinogen. Interestingly, R149Q and R173Q mutations of human PBGD have been reported to inactivate the enzyme (32). The amide nitrogen of R149 is seen forming a 2.8 Å hydrogen bond with the carboxyl oxygen of the acetic acid side chain, while the amide nitrogen of R173 is seen forming a 2.7 Å hydrogen bond with the carboxyl oxygen of the propionic acid side chain of the C1 ring of the dipyrromethane cofactor (Fig. 6*A*). These interactions are critical for the optimal docking of porphobilinogen into the active site. R149Q and R173Q mutations result in an apo form of the enzyme incapable of catalysis. Another mutation involving an arginine residue, R167Q, has been reported to compromise the enzyme activity (32). This mutation does not affect the ability of the enzyme to form intermediate complexes with substrate molecules, but prolongs the release of the product from the active site. Analysis of the structure reveals R167 sitting on a loop at the edge of the active site cleft. Although R167 is far away from the cofactor, a R167Q mutation in the loop may sterically block the release of the final product.

DISCUSSION

Role of hinge regions

Once PBGD assumes the holoenzyme conformation, the dipyrromethane cofactor remains permanently at-
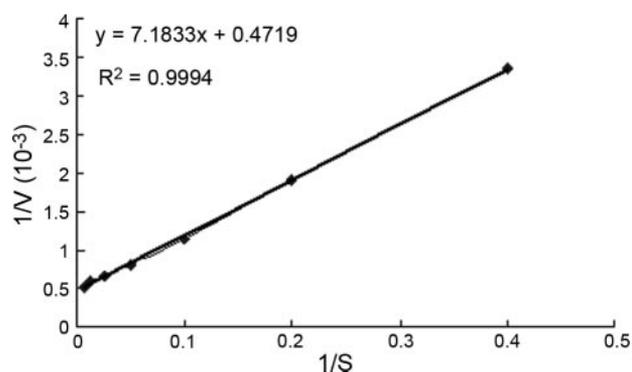

Figure 4. Lineweaver-Bruke plot of human PBGD. The enzyme had a V_{max} of 2110 U/mg and K_m of 15.3 μM when assayed under the conditions described in Materials and Methods.

Figure 5. Schematic of mechanism of substrate catalysis of PBGD. Porphobilinogen is deaminated to methylene pyrrolinene, and the free α position on the C2 ring of the cofactor, on activation by D99, forms a carbon-carbon bond with the methylene pyrrolinene. After stabilization of the intermediate ES1, the reaction proceeds through ES2, ES3, and ES4 stages, with the addition of a pyrrole ring at each stage in a similar fashion.
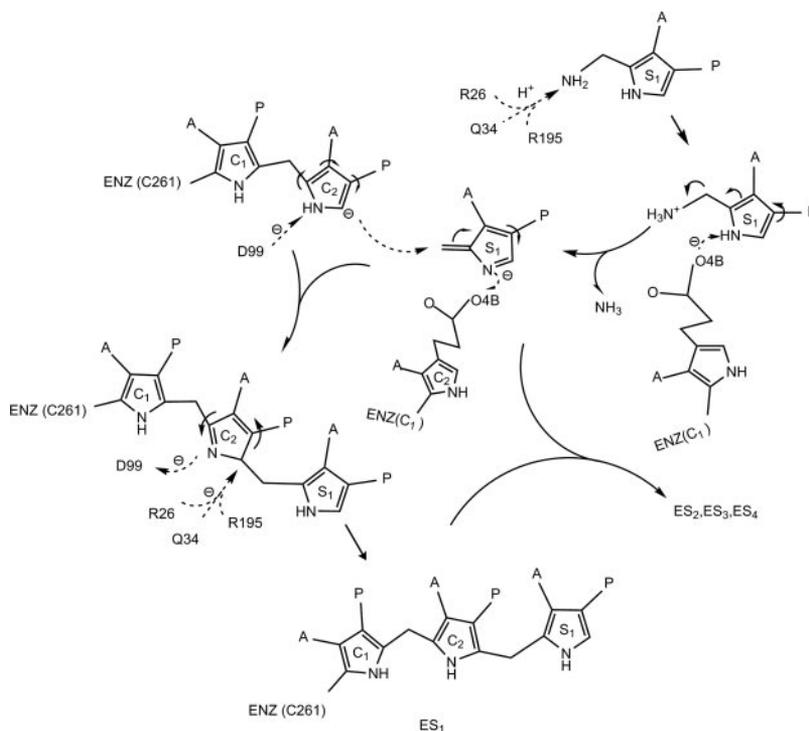
tached to the enzyme and is never turned over during subsequent catalysis. The cofactor acts like a template on which new pyrrole rings are added. Assembly of the tetrapyrrole product has been postulated to proceed in discreet sequential steps. At least 4 reaction intermediates, ES1, ES2, ES3, and ES4, each depicting the sequential fusion of a pyrrole ring have been biochemically characterized (15, 16). As soon as a pryrrole ring enters the active site, it is isolated from its immediate environment and fused to the aromatic ring of the cofactor containing a free carbon at the α-position. The reaction proceeds with the addition of 3 more pyrrole rings in a similar fashion. For such a mechanism to be possible, it requires the enzyme to be flexible such that the active site is open for the entry of a new pyrrole molecule and closed during the ring fusion. Such opening and closing of the active site in human PBGD is accomplished by movement of domains 1 and 2 around the hinge regions. We used HingeProt (33) to predict the putative hinge regions in human PBDG that could assist the opening and closure of the active site. HingeProt identified S96, H120, and L238 as hinge residues, around which the domains move (**Fig. 7**). S96 is positioned at the bottom edge of domain 1 and is at the interface of domains 1 and 3. Similarly, H120 is positioned at the bottom edge of domain 2 and is at the interface of domains 2 and 3. Domain 1 and 2 probably swing outside and away from each other around these hinge residues, resulting in the opening of the active site. A reverse movement would result in closure of the active site. L238 is positioned in the middle of the protein, close to the point where the interfaces of all the 3 domains converge. The movement of domain 1 seems to be centered around this hinge residue. Mutations of hinge residues S96F and L238R, reported in patients

suffering from AIP, result in decreased PBGD activity (Supplemental Table 1). To confirm the role of H120 as a hinge residue, we performed H120A and H120P mutations. The mutant enzyme could be purified similar to the wild type and showed an identical size-exclusion chromatography profile as the wild type. While the H120A mutation had no effect on the enzyme activity, interestingly, a H120P mutation resulted in an inactive enzyme. H120 is far away from the active site and is not seen interacting with any other residue. Mutation of H120 to alanine does not affect the ability of this region to function like a hinge, and therefore, this mutation did not affect the enzyme activity. However, a H120P mutation makes this region rigid, preventing any movement. Therefore, the H120P mutant enzyme lost its activity, thereby supporting the role of H120 as a hinge residue. Further, four short segments, 116–118, 106–111, 147–156, and 206–221, were predicted as flexible fragments by HingeProt. The flexible fragments, 116–118 and 206–221, are located on loops running in opposite direction at the bottom center of the active site and are seen connecting domain 1 with domain 2. Residues 106 and 107 from the flexible segment 106–111 are part of a loop region, while the remaining residues are seen forming the β4 sheet. This flexible fragment is located at the interface of domain 1 and domain 3. The flexible fragment made up of residues 147-156 is positioned at the interface of domains 2 and 3. These flexible fragments are likely to assist the movement of the domains while keeping the secondary structure of the protein intact by acting like "shock-absorbers" and neutralizing the force generated during the movement of the domains. The movement of the domains around the hinge regions during catalysis is depicted in Supplemental Video 1. Similar hinge
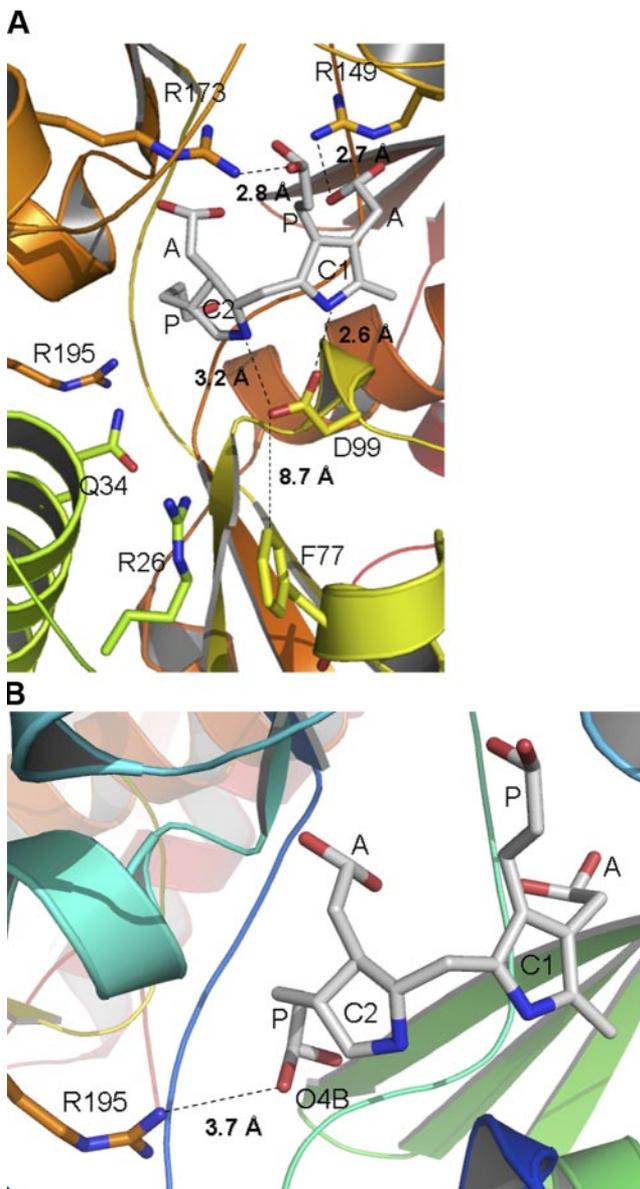
Figure 6. Critical residues for catalysis. D99 is seen forming hydrogen bonds with the C1 and C2 rings of dipyrromethane cofactor. Unlike the PBGD from *E. coli*, F77 in human PBGD is not in a position to protonate D99. Protonation of the incoming porphobilinogen could be carried out by positively charged residues positioned close to the C2 ring. The carboxylate of the propionate side chain of C2 ring is seen forming a weak interaction with R195NH1. Density for the O4 atom of the propionate side chain of the C2 ring is not visible in chain B (*A*), but is distinct in chain A (*B*). Acetate and propionate side chains are labeled as A and P, respectively.

movements have been reported before for phenylalanine hydroxylase, transferrins and have been indicated in PBGD from *E. coli* (17, 34, 35, 36).

Mapping mutations of AIP patients

A number of mutations have been documented in the PBGD gene of patients suffering from AIP. These mutations lead to a variety of consequences, such as loss of the transcript, splicing defects, frameshifts, trunca-

TABLE 2. *Relative activity of PBDG mutants*

Mutation	Relative activity (%)
Wild type	100
R26A	1.1
Q34A	4.8
R195A	NA
H120A	91
H120P	1.9

NA, no activity.

tion of the protein, and denaturation or amino acid substitutions in the enzyme (37). To understand the structural and functional consequences of mutations involving amino acid substitutions, we mapped their location on the structure of human PBGD. **Figure 8** shows the location of 81 amino acid substitutions documented in the PBGD genes of patients suffering from AIP. Although the type of amino acid substitution and location could vary considerably, all mutations have deleterious effects on enzyme activity (37). Interestingly, some of the mutations are located far away from the active site. Amino acid substitutions K98R, R149Q, R173W, R195C, and Q217L, resulting in loss of enzyme activity, can be explained by the fact that these amino acids are located inside the active site cleft and are in close vicinity of the dipyrromethane cofactor. They are probably critical for docking of the substrate molecules and catalysis. These mutations do not affect
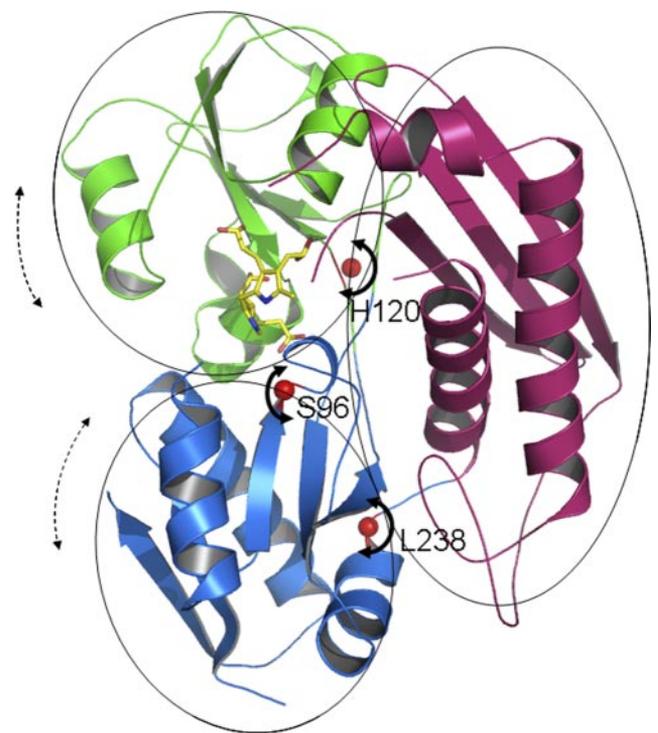
Figure 7. Model of PBGD depicting the movement of domains around the hinge regions. Hinge residues S96, H120, and L238, predicted by HingeProt, are shown as red balls. Arrows indicate movement of domains. Cofactor is shown as sticks.
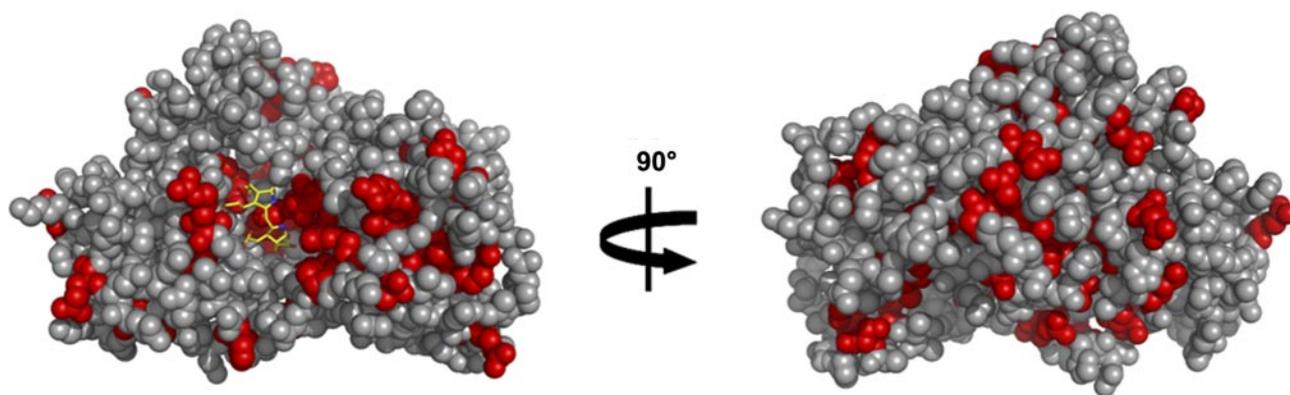
Figure 8. Mapping of single amino acid substitutions as a result of mutations in the *PBGD* gene. Red balls represent amino acids substituted in the PBGD of patients suffering from AIP. For a complete list of mutations, see Supplemental Table 1.

the folding and stability of the enzyme, and therefore, the patients are cross-reacting immunoreactive material (CRIM) positive. Mutations far away from the active site could be deleterious because they affect either the folding of the protein and its stability or the ability of the domains to move around the hinge regions. R116W, R225G, and L278P mutations result in CRIM-negative phenotype. These mutations probably disrupt the secondary structure of the polypeptide. R116 is positioned at the bottom of the active site on a loop linking domain 1 with domain 2. It is seen forming a number of interactions with residues from domain 1 and domain 2. R116W mutation disrupts these favorable interactions and destabilizes the protein. R225 is located at the edge of domain 1 and is seen forming ionic interactions with N88 and D228. R225G mutation abolishes these stabilizing ionic interactions. L278 is located in the hydrophobic core of domain 3 and a L278P mutation probably destabilizes the core. Mutations like S96F and L238R, which are far away from the active site, result in inactivation of PBGD possibly due to the inability of domain 1 and domain 2 to swing around these hinge residues in order to allow the entry of new substrate molecules into the active site. Although the mutations could be mapped at different locations, not surprisingly, the clinical manifestations reported for these mutations are uniform (37). This could be because of the fact that all the mutations reported so far result in a decrease of PBGD activity, and the symptoms of AIP have been linked to lower levels of PBGD activity. An updated list of the amino acid substitutions documented in AIP patients is shown in Supplemental Table 1.

The structure of phenylalanine hydroxylase (PAH) has been studied similarly in case of another metabolic disorder, phenylketonuria (PKU) (34, 35), and has been successfully used to develop therapeutics. Symptoms of PKU have been linked to decreased activity of PAH as a result of mutations in the *PAH* gene. Kuvan, an FDA-approved drug for the treatment of tetrahydrobiopterin (BH4) -responsive PKU, has been shown to stimulate the residual activity of PAH in PKU patients (38), while preliminary results of an enzyme replacement therapy for the treatment of PKU carried out in

mice have been very encouraging (39). A similar strategy aimed at enhancing the activity of PBGD by using a small molecule or enzyme replacement therapy could help alleviate the symptoms of AIP.

In summary, we have determined the 3-D structure of human PBGD at 2.2 Å resolution. A dipyrromethane cofactor molecule bound to the protein could help gain insights into the active site architecture and identify critical residues for catalysis. Predicted hinge regions of PBGD seem to play a critical role in the assembly of the terrapyrrole product. Mutagenesis studies support the role of H120 as a potential hinge residue. Amino acid substitutions reported in AIP patients could be mapped on the structure. The implications of such mutations on the structure and function of the enzyme could be interpreted by analyzing the structure. The structure of PBGD in ES1, ES2, ES3, and ES4 transition states of catalysis could eventually unravel the complete mechanism of synthesis of preuroporphyrinogen. This work is currently under way. **FJ**

REFERENCES

1. Furuyama, K., Kaneko, K., and Vargas, P. D. 5th (2007) Heme as a magnificent molecule with multiple missions: heme determines its own fate and governs cellular homeostasis. *Tohoku J. Exp. Med.* **213,** 1–16
2. Granick, S., and Beale, S. I. (1978) Hemes, chlorophylls, and related compounds: biosynthesis and metabolic regulation. *Adv. Enzymol. Relat. Areas Mol. Biol.* **46,** 33–203
3. Kauppinen, R. (2005) Porphyrias. *Lancet* **365,** 241–252

4. Anderson, K., Sassa, S., Bishop, D., and Desnick, R. (2001) Disorders of heme biosynthesis: X-linked sideroblastic anemia and the porphyrias. In *The Metabolic and Molecular Basis of Inherited Disease* (Scriver, C. R., Beaudet, A. L., Sly, W. S., and Valle, D., eds) pp. 2991–3062, McGraw-Hill, New York, NY, USA

5. Woodard, S. I., and Dailey, H. A. (2000) Multiple regulatory steps in erythroid heme biosynthesis. *Arch. Biochem. Biophys.* **384,** 375–378

6. Woodard, S. I., and Dailey, H. A. (1995) Regulation of heme biosynthesis in *Escherichia coli. Arch. Biochem. Biophys.* **316,** 110–115

7. Meyer, U. A., and Schmid, R. (1978) The porphyrias. In *The Metabolic Basis of Inherited Disease* (Stanbury, J. B., Wyngaarden, J. B., and Fredrickson, D. S., eds) pp. 1166–1220, McGraw-Hill, New York, NY, USA

8. Kappas, A., Sassa, S., Galbraith, R. A., and Nordmann, Y. (1995) The porphyrias. In *The Metabolic and Molecular Basis of Inherited Diseases* (Scriver, C. R., Beaudet, A., Sly, W. S., and Valle, D., eds) pp. 2116–2127, McGraw-Hill, New York, NY, USA

9. Grandchamp, B. (1998) Acute intermittent porphyria. *Semin Liver Dis.* **18,** 17–24

10. Puy, H., Deybach, J. C., Lamoril, J., Robreau, A. M., Silva, V. D., Gouya, L., Grandchamp, B., and Nordmann, Y. (1997) Molecular epidemiology and diagnosis of PBG deaminase gene defects in acute intermittent porphyria. *Am. J. Hum. Genet.* **60,** 1373–1383

11. Strand, L. J., Meyer, U. A., Felsher, B. F., Redeker, A. G., and Marver, H. S. (1972) Decreased red cell uroporphyrinogen I synthetase activity in intermittent acute porphyria. *J. Clin. Invest.* **51,** 2530–2536

12. Kauppinen, R., and Mustajoki, P. (1992) Prognosis of acute intermittent porphyria: occurrence of acute attacks, precipitating factors and associated disease. *Medicine* **71,** 1–13

13. Grandchamp, B., Verneuil, H. D., Beaumont, C., Chretien, S., Walter, O., and Nordmann, Y. (1987) Tissue-specific expression of porphobilinogen deaminase: two isoenzymes from a single gene. *Eur. J. Biochem.* **162,** 105–110

14. Jordan, P. M. (1996) Biosynthesis of tetrapyrroles. In *New Comprehensive Biochemistry* (Neuberger, A., and Van Deenen, L. L. M., eds) pp. 1–66, Elsevier, Amsterdam, The Netherlands

15. Warren, M. J., and Jordan, P. M. (1988) Investigation into the nature of substrate binding to the dipyrromethane cofactor of *Escherichia coli* porphobilinogen deaminase. *Biochemistry* **27,** 9020–9030

16. Anderson, P. M., and Desnick, R. J. (1980) Purification and Properties of uroporphyrinogen I synthase from human erythrocytes. *J. Biol. Chem.* **225,** 1993–1999

17. Louie, G. V., Brownlie, P. D., Lambert, R., Cooper, J. B., Blundell, T. L., Wood, S. P., Warren, M. J., Woodcock, S. C., and Jordan, P. M. (1992) Structure of porphobilinogen deaminase reveals a flexible multidomain polymerase with a single catalytic site. *Nature* **359,** 33–39

18. Stols, L., Gu, M., Dieckman, L., Raffen, R., Collart, F. R., and Donnelly, M. I. (2002) A new vector for high-throughput, ligation-independent cloning encoding a tobacco etch virus protease cleavage site. *Protein Expr. Purif.* **25,** 8–15

19. Otwinowski, Z., and Minor, W. (1997) Processing of X-ray diffraction data collected in oscillation mode. *Methods Enzymol.* **276,** 307–326

20. Long, F., Vagin, A., Young, P., and Murshudov, G. (2008) BALBES: a molecular-replacement pipeline. *Acta Crystallogr. D* **64,** 125–132

21. Adams, P. D., Grosse-Kunstleve, R. W., Hung, L. W., Ioerger, T. R., McCoy, A. J., Moriarty, N. W., Read, R. J., Sacchettini, J. C., Sauter, N. K., and Terwilliger, T. C. (2002) PHENIX: building new software for automated crystallographic structure determination. *Acta Crystallogr. D* **58,** 1948–1954

22. Emsley, P., and Cowtan, K. (2004) Coot: model-building tools for molecular graphics. *Acta Crystallogr. D* **60,** 2126–2132

23. Combet, C., Jambon, M., Deléage, G., and Geourjon, C. (2002) Geno3D: automatic comparative molecular modelling of protein. *Bioinformatics* **18,** 213–214

24. Jones, R. M., and Jordan, P. M. (1994) Purification and properties of porphobilinogen deaminase from *Arabidopsis thaliana. Biochem. J.* **299,** 895–902

25. Correa-Garcia, S. R., Rossetti, M. V., and Batile, A. M. (1991) Studies on porphobilinogen-deaminase from *Saccharomyces cerevisiae. Z. Naturforsch. C.* **46,** 1017–1023

26. Jordan, P. M., Thomas, S. D., and Warren, M. J. (1988) Purification, crystallization and properties of porphobilinogen deaminase from a recombinant strain of *Escherichia coli* K12. *Biochem. J.* **254,** 427–435

27. Mazzetti, M. B., and Tomio, J. M. (1988) Characterization of porphobilinogen deaminase from rat liver. *Biochim. Biophys. Acta* **957,** 97–104

28. Jordan, P. M., and Shemin, D. (1973) Purification and properties of uroporphyrinogen I synthetase from *Rhodopseudomonas spheroides. J. Biol. Chem.* **248,** 1019–1024

29. Brons-Poulsen, J., Christiansen, L., Petersen, N., Horder, M., and Kristiansen, K. (2005) Characterization of two isoalleles and three mutations in both isoforms of purified recombinant human porphobilinogen deaminase. *Scand. J. Clin. Lab. Invest.* **65,** 93–105

30. Jordan, P. M., Warren, M. J., and Awan, S. J. (1996) Discovery that the assembly of the dipyrromethane cofactor of porphobilinogen deaminase holoenzyme proceeds initially by the reaction of preuroporphyrinogen with the apoenzyme. *Biochem. J.* **316,** 373–376

31. Woodcock, S. C., and Jordan, P. M. (1994) Evidence for participation of aspartate-84 as a catalytic group at the active site of porphobilinogen deaminase obtained by site-directed mutagenesis of the *hemC* gene from *Escherichia coli. Biochemistry* **33,** 2688–2695

32. Jordan, P. M., Al-Dbass, A., McNeill, L. A., Sarwar, M., and Butler, D. (2003) Human porphobilinogen deaminase mutations in the investigation of the mechanism of dipyrromethane cofactor assembly and tetrapyrrole formation. *Biochem. Soc. T.* **31,** 731–735

33. Emekli, U., Schneidman-Duhovny, D., Wolfson, H. J., Nussinov, R., and Haliloglu, T. (2007) HingeProt: automated prediction of hinges in protein structures. *Proteins* **70,** 1219–1227

34. Erlandsen, H., Fusetti, F., Martinez, A., Hough, E., Flatmark, T., and Stevens, R. C. (1997) Crystal structure of the catalytic domain of human phenylalanine hydroxylase reveals the structural basis for phenylketonuria. *Nat. Struc. Mol. Biol.* **4,** 995–1000

35. Fusetti, F., Erlandsen, H., Flatmark, T., and Stevens, R. C. (1998) Structure of tetrameric human phenylalanine hydroxylase and its implications for phenylketonuria. *J. Biol. Chem.* **273,** 16962–16967

36. Anderson, B. F., Baker, H. M., Norris, G. E., Rumball, S. V., and Baker, E. N. (1990) Apolactoferrin structure demonstrates ligand-induced conformational change in transferrins. *Nature* **344,** 784–787

37. Hrdinka, M., Puy, H., and Martasek, P. (2006) May 2006 update in porphobilinogen deaminase gene polymorphisms and mutations causing acute intermittent porphyria. Comparison with the situation in Slavic population. *Physiol. Res.* **55,** 119–136

38. Matalon, R., Michals-Matalon, K., Koch, R., Grady, J., Tyring, S., and Stevens, R. C. (2005) Response of patients with phenylketonuria in the US to tetrahydrobiopterin. *Mol. Genet. Metab.* **86**(Suppl. 1), 17–21

39. Gamez, A., Wang, L., Sarkissian, C. N., Wendt, D., Fitzpatrick, P., Lemontt, J. F., Scriver, C. R., and Stevens, R. C. (2007) Structure-based epitope and PEGylation sites mapping of phenylalanine ammonia-lyase for enzyme substitution treatment of phenylketonuria. *Molec. Genet. Metab.* **91,** 325–334